JPn Neuroscience
The Journal of Physiology

J Physiol 0.0 (2015) pp 1–13

SYMPOSIUM REVIEW

Non-signalling energy use in the brain

Elisabeth Engl and David Attwell

Department of Neuroscience, Physiology & Pharmacology, University College London, London WC1E 6BT, UK

Abstract Energy use limits the information processing power of the brain. However, apart from the ATP used to power electrical signalling, a significant fraction of the brain's energy consumption is not directly related to information processing. The brain spends just under half of its energy on non-signalling processes, but it remains poorly understood which tasks are so energetically costly for the brain. We review existing experimental data on subcellular processes that may contribute to this non-signalling energy use, and provide modelling estimates, to try to assess the magnitude of their ATP consumption and consider how their changes in pathology may compromise neuronal function. As a main result, surprisingly little consensus exists on the energetic cost of actin treadmilling, with estimates ranging from < 1% of the brain's global energy budget up to one-half of neuronal energy use. Microtubule treadmilling and protein synthesis have been estimated to account for very small fractions of the brain's energy budget, whereas there is stronger evidence that lipid synthesis and mitochondrial proton leak are energetically expensive. Substantial further research is necessary to close these gaps in knowledge about the brain's energy-expensive non-signalling tasks.

(Received 13 August 2014; accepted after revision 27 January 2015; first published online 29 January 2015)
Corresponding author D. Attwell: Department of Neuroscience, Physiology & Pharmacology, University College London, Gower Street, London WC1E 6BT, UK. Email: d.attwell@ucl.ac.uk

Abbreviations CBF, cerebral blood flow; CSD, cortical spreading depression; $CMRO_2$, cerebral metabolic rate of oxygen; PARP, poly(ADP-ribose) polymerase.

Introduction

The human brain is only 2% of the body's mass but uses 20% of its resting energy production (Kety, 1957; Sokoloff, 1960; Rolfe & Brown, 1997). Theoretical energy budgets for the brain, based on experimental measurements, have established that this disproportionate energy use largely reflects the energetic cost in neurons of pumping out sodium ions that enter to generate synaptic and action potentials (Attwell & Laughlin, 2001; Lennie, 2003; Harris & Attwell, 2012). This large energy use constrains the information processing power of the brain and determines key parameters affecting brain function, including the mean firing rate of neurons, the release probability of synapses and the physical size of synaptic contacts (Laughlin & Sejnowski, 2003; Lennie, 2003; Attwell & Gibb, 2005; Niven & Laughlin, 2008; Harris *et al.* 2012). As a result, it has been hypothesised that the high energetic demands of neurons are partly met by energy production in neighbouring glial cells, both astrocytes and oligodendrocytes (Pellerin & Magistretti, 1994; Nave, 2010; Fünfschilling *et al.* 2012).

Elisabeth Engl is currently in her final year of the Wellcome Trust 4-year PhD Programme in Neuroscience at University College London, working on brain and synaptic energy use in David Attwell's lab. Her interests lie in energetic constraints on information processing and brain function. She has also previously worked in cognitive neuroscience at UCL, MIT and the University of Vienna, and was a pianist in her former life. **David Attwell** started out in Oxford as a physicist, before switching to the electrophysiology of nerve and muscle for his PhD. After a post-doc in Berkeley working on the retina, he was recruited to UCL where he is now the Jodrell Professor of Physiology. He has worked on diverse topics including neuron-glial interactions, glutamate transporters and brain energy use.


This review was presented at the symposium *Coupling Cellular Metabolism to Neuronal Signalling*, which took place at Physiology 2014, the annual meeting of The Physiological Society, London, UK on 1 July 2014.

 DOI: 10.1113/jphysiol.2014.282517

Perhaps surprisingly, a significant fraction of brain energy use (25–50%) in previous energy budgets has been assigned to non-signalling (so-called 'housekeeping') tasks, which include protein and lipid synthesis, proton leak across the mitochondrial membrane, and cytoskeletal rearrangements, the rate of ATP consumption on all of which is poorly understood. The energetic consumption of these processes must contribute to limiting the cognitive abilities of the brain because the total energy use of the brain constrains the temporal rate at which information can be encoded and processed (Attwell & Gibb, 2005). Accepting the (poorly substantiated) view that 'housekeeping' consumes ∼25% of the brain's ATP, if this could be (say) halved then the energy available for information processing would rise by 17%, giving animals with reduced 'housekeeping' costs a cognitive advantage (although it could be argued that it is unclear to what extent 'housekeeping' processes can be made more energy efficient by evolution because they provide the conditions essential for normal neuronal function). Conversely, a common pathology, ischaemia, by inhibiting the sodium-potassium pump, loads cells with ions that need to be pumped out when blood flow is restored, and DNA damage caused by peroxynitrite release after ischaemia leads to activation of the poly(ADP-ribose) polymerase (PARP) pathway (Pacher & Szabo, 2008), both of which increase ATP use (Ha & Snyder, 2000). Increased ATP use on these restorative processes presumably deprives signalling processes of energy, and thus compromises information processing power, although the quantitative significance of such energetic changes in pathology is unknown.

Here, we review the possible subcellular mechanisms that may contribute to non-signalling ATP consumption in the brain, assess their probable relative importance and consider the implications of changes in non-signalling energy use in pathology.

Results

The sodium-potassium pump is a major energy drain

In rabbit brain slices, Whittam (1961) measured a fall in oxygen consumption of 50% after inhibiting (with ouabain) the sodium-potassium pump, which pumps three sodium ions out of a cell in exchange for shuttling two potassium ions into it. Similarly, using a Clark-type oxygen electrode, Shibuki (1989) observed an immediate rise in the baseline oxygen level of ∼28 mmHg (i.e. 16% of the resting level) in the rat neurohypophysis after the application of ouabain. In a seminal *in vivo* study on dogs, Astrup *et al.* (1981*a*) quantified the energy used on the sodium-potassium pump more precisely. Using a combination of pentobarbital and lidocaine to reduce Na^+ influx, and ouabain to block the sodium-potassium pump, they found that sodium pumping was responsible for 55% of the brain's oxygen usage, relative to the oxygen use in animals anaesthetised with halothane (recalculated from Astrup *et al.* 1981*a*). Assuming that halothane reduces neuronal firing, and thus reduces sodium entry into cells, this implies that, in unanaesthetised animals, sodium pumping accounts for more than 55% of ATP use, and less than 45% is used on other tasks. If we assume, for simplicity, that Na^+ pumping is exclusively used to power signalling (including maintenance of the resting potential), then $<$ 45% of ATP is used on non-signalling tasks.

Theoretical work by Attwell & Laughlin (2001), which was later updated by Harris & Attwell (2012) to correct for the lower sodium influx by then reported to occur during action potentials (Alle *et al.* 2009; but see also Hallermann *et al.* 2012), complemented this experimental work by calculating the amount of ATP used on different signalling-related mechanisms in neurons firing at a physiological rate of 4 Hz. This analysis used experimental data to evaluate the Na^+ and Ca^{2+} influxes that generate action potentials and synaptic currents, and occur at the resting potential, and then converted those fluxes to the amount of ATP used on Na^+ and Ca^{2+} pumping. The number of sodium ions needed to charge the capacitance of an unmyelinated cortical axon and to depolarise the cell body and dendrites to produce the voltage changes that occur during an action potential was calculated. The number of ATP molecules the sodium-potassium pump requires to pump out those Na^+ ions after an action potential (one-third of the Na^+ influx) could thus be determined, and scaled to give the tissue expenditure on action potentials. This was 23% of the signalling-related energy use and 17% of the total energy expenditure in the grey matter (assuming 25% of total energy is spent on 'housekeeping' processes, consistent with the estimate from the sodium pump data of Astrup *et al.* (1981*a*) indicating that processes unrelated to signalling use less than 45% of the ATP), but was only 0.4% of the total energy use in fully myelinated white matter (Harris & Attwell, 2012; Attwell & Laughlin, 2001). Postsynaptic ion fluxes through ionotropic AMPA and NMDA receptors, the ATP used on postsynaptic G protein-coupled receptors, presynaptic Ca^{2+} entry triggering vesicle release and presynaptic ATP use on vesicle cycling were estimated from patch-clamp and calcium imaging data in the literature. These were estimated to consume 43% of ATP use in the grey matter but only 0.1% in the white matter, where 'housekeeping' processes and ion pumping to maintain the resting potential comprise the majority of energy use (Harris & Attwell, 2012; Attwell & Laughlin, 2001). Finally, from the membrane resistance and resting potential of a typical neuron, the leak conductances for sodium and potassium were derived, allowing calculation of the number of ATP molecules needed to power the sodium

pump to reverse the resting ion fluxes. This led to the ATP used to maintain the resting potential being estimated as 15% of the total energy use in the grey matter and 44% in the white matter (Harris & Attwell, 2012; Attwell & Laughlin, 2001).

Sibson *et al.* (1998) attributed a higher percentage (>80%) of energy expenditure to synaptic and action potential signalling than the 60% suggested by Harris & Attwell (2012). In the rodent cortex, they measured the rate of conversion of glutamate into glutamine, which they interpreted as glutamate recycling through astrocytes and therefore used it as a proxy of synaptic activity, and deduced the rate of glucose consumption from the citric acid cycle rate. Sibson *et al.* (1998) found that high anaesthesia levels reduced the rate of conversion from glutamate to glutamine to zero, whereas the rate of glucose consumption was only reduced by > 80%. These data were interpreted as meaning that ∼20% of energy expenditure are spent on events not related to glutamate release (i.e. 'housekeeping'). However, the approach of Sibson *et al.* (1998) rested on a set of assumptions regarding the K_m for transporters, a lack of exchange between neuronal glutamate and glutamine pools, and an assumption that, for two of the anaesthetics used in their experiments, it was neuronal glutamate that is used to make glutamine, whereas for the third anaesthetic, it was glial glutamate. Furthermore, conclusions from these data depend critically on how anaesthetics affect different energy-consuming mechanisms in the brain. Because of these assumptions, interpretation of the data obtained by Sibson *et al.* (1998) remains uncertain.

Together, these results demonstrate that a high percentage of ATP use is spent on signalling-related processes such as reversing sodium entry after action potentials, synaptic ion fluxes, and maintaining the resting membrane potential. However, non-signalling processes must also use a substantial amount of ATP to explain the difference between the energy used on the sodium pump and the total brain energy consumption (Fig. 1): for the grey matter of rat neocortex, Harris & Attwell (2012) estimated an ATP use of 21 μmol g^{-1} min^{-1} on signalling processes, whereas experimental measurements of total ATP use are in the range 30–50 μmol g^{-1} min^{-1} (McKenna *et al.* 2012).

The actin cytoskeleton undergoes continuous treadmilling

A likely candidate for substantial energy expenditure on 'housekeeping' tasks is the actin cytoskeleton present in all eukaryotic cells. It is responsible for the maintenance of, and changes in, cell morphology, as well as cell division and motility (Condeelis, 1993; Carlier & Pantaloni, 1997; Hall, 1998; Pollard & Borisy, 2003). The actin cytoskeleton undergoes a continuous cycle of polymerisation (from G-actin monomers to long F-actin polymers) and depolymerisation (Wegner, 1976), as shown in Fig. 2. This 'treadmilling' is dependent on ATP hydrolysis (Carlier *et al.* 1988; Belmont & Drubin, 1998).

The mechanisms that regulate the turnover rate of actin, including a complex array of proteins, as well as parameters such as the proportion of free G-actin to F-actin bound in filaments, are highly conserved across eukaryotic phyla (Pollard *et al.* 2000). F-actin filaments are constructed by the reversible addition of monomers to both ends but one end (the 'barbed' or 'plus' end) elongates 5 to 10 times faster than the 'minus' end: ∼0.3 μm s^{-1} at a concentration of 10 μM actin monomers, which is at the low end of the typical intracellular concentration (Pollard & Borisy, 2003). During treadmilling, G-actin monomers with bound ATP thus attach mainly to the plus end of F-actin, where hydrolysis of ATP occurs. Phosphate is released and the G-actin molecules incorporated into F-actin now have ADP bound to them. At the minus end, G-actins binding ADP are disassembled from the main strand of F-actin, and ADP is exchanged for ATP as the monomer awaits re-attachment to the plus end of F-actin (Pantaloni *et al.* 2001). The rate of ATP consumption is proportional to the rate of treadmilling (Bernstein & Bamburg, 2003). However, different structural states of the actin filaments also play a role in turnover, with newer filaments being in more unstable configurations than older ones and therefore depolymerising more rapidly (Kueh & Mitchison, 2009).

Bernstein and Bamburg (2003) determined the amount of ATP used by the actin cytoskeleton by blocking ATP synthesis in cultured neurons and measuring the resulting fall of ATP concentration to deduce the rate of ATP use. Slowing actin filament turnover with jasplakinolide, which prevents F-actin depolymerisation, halved the rate of ATP depletion compared to when the cytoskeleton was not stabilised, suggesting that half of the neurons' ATP usage was on actin cycling. It was also found that the other 50% of the ATP depletion was blocked by inhibiting the sodium pump with ouabain, apparently implying that actin cycling uses as much ATP as (mainly signalling-related) Na^+ pumping. However, this energy deprivation approach to measuring ATP use will result in adenosine being released, and therefore glutamate release being suppressed (Fowler, 1990; Fowler, 1993*a*, 1993*b*; Latini *et al.* 1998), which will decrease the large amount of ATP used on postsynaptic currents and downstream action potentials. Thus, this approach to assessing the amount of ATP used on actin treadmilling may be confounded by a greatly decreased rate of ATP use on synaptic and action potential signalling, increasing artefactually the fraction of ATP that appears to be used on actin cycling.

Reinforcing this view, quantitative assessment of the role of actin turnover raises the possibility that very little energy is actually used on actin treadmilling. Almost all

actin in dendrites (81.4%) turns over every 44 s, with 14% of actin being in the form of free G-actin monomers and only 4.6% being stable actin (Star *et al.* 2002). For a typical total monomeric actin concentration (in G- and F-actin) of ∼100 μM (Devineni *et al.* 1999), then (81.4/100) × (100 μM/44 s) = 1.8 μM ATP s^{-1} is used to turn over actin (or 5.4 μM ATP s^{-1} using instead the data of Pathania *et al.* (2014) who found that 70% turns over with a time constant of 13 s). Assuming this is similar for all cell types in the brain, and taking account of the 20% extracellular space that does not contain actin, this implies a spatially averaged value of 1.5 μM ATP s^{-1}. In non-anaesthetised rats, grey matter uses 16.7 μM glucose s^{-1} or 516 μM ATP s^{-1} if 31 ATP molecules are assumed to be made per glucose (Sokoloff *et al.* 1977). Therefore, only a very small fraction of the brain's total ATP use (1.5 μM s^{-1})/(516 μM s^{-1}), which is 0.29% (or 0.9% using the data of Pathania *et al.* (2014)), is predicted to be spent on actin turnover. The turnover time of 44 s was observed under conditions where neurons fired spontaneously at 0.5 Hz (Star *et al.* 2002). Abolishing all synaptic transmission with TTX reduced the turnover time to 32.8 s and increased treadmilling actin to 85.4% of all actin. However, this still suggests that only 0.4% of all ATP is used on actin cycling. Conversely, stimulating at 1 Hz resulted in a slower turnover time (52.2 s) and reduced actin treadmilling (45%). In this case, only 0.13% of the brain's ATP would be spent on actin cycling. Substituting the value of 200 μM ATP s^{-1} reported by Purdon & Rapoport (2007) in the rat brain for the value of 516 μM s^{-1} reported by Sokoloff *et al.* (1977) more than doubles these percentage estimates but, even then, they would remain an extremely small contribution to the brain's overall energy budget.

One possible reconciliation between the results obtained by Bernstein and Bamburg (2003) and these very

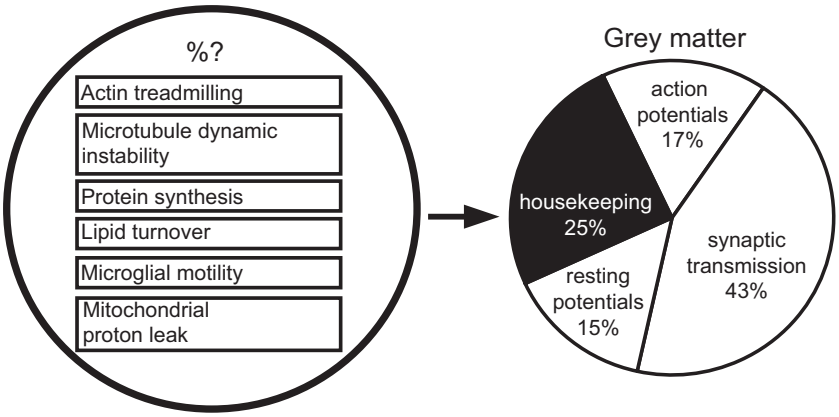

Figure 1. Energy budget for the grey matter adapted fromHarris & Attwell (2012)
For the grey matter, Attwell & Laughlin (2001) and Harris & Attwell (2012) assumed that 'housekeeping' processes account for 25% of total energy use (right diagram shows numbers from Harris & Attwell, 2012). Assuming the same housekeeping energy use per unit volume, Harris & Attwell (2012) showed that this would be ∼60% of total energy use in the white matter where far less energy is spent on synaptic transmission and action potentials. Under the umbrella term of 'housekeeping', the brain carries out many distinct processes (left). Their relative contributions to the total energy budget, and the balance of 'housekeeping' and signalling energy expenditure in the brain, are reviewed.

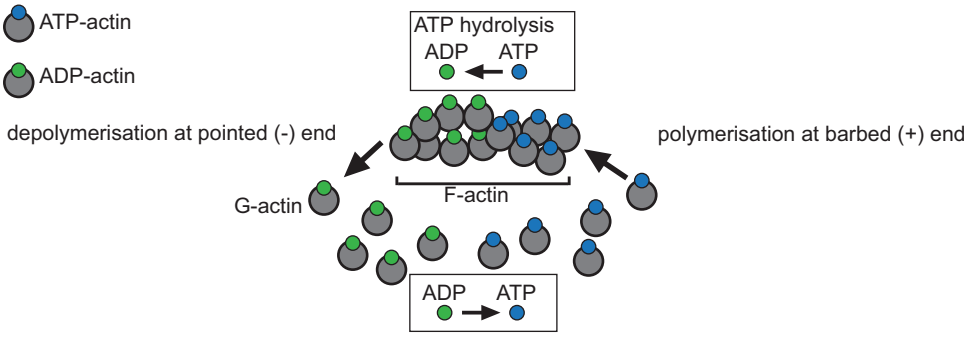

Figure 2. Continuous ATP-dependent treadmilling of the actin cytoskeleton
Exchanging the ADP bound to free G-actin monomers for ATP enables them to bind (predominantly) to the barbed end of actin filaments, causing them to grow. The bound ATP is subsequently hydrolysed and ADP-bound actin monomers can then detach from the pointed end of the filament, completing the cycle.

small projections of actin ATP use would be that turnover times might be shorter in areas other than dendrites, or in cells other than neurons. Alternatively, pools of filaments smaller than those studied by Star *et al.* (2002), turning over much faster, might lead to a much higher rate of ATP use. To resolve this issue more definitively, further experimental evidence is needed.

'Housekeeping' as a foundation for signalling: the example of vesicle cycling

'Housekeeping' tasks may also consume energy during signalling. For example, presynaptic vesicle cycling, which may involve actin rearrangements and actin-based transport (Sankaranarayanan *et al.* 2003; Shupliakov *et al.* 2002), has been suggested to be an energetically expensive process (Rangaraju *et al.* 2014). Rangaraju *et al.* (2014) found that, in hippocampal synaptic terminals, with ATP synthesis inhibited with oligomycin or 2-deoxyglucose, 60 s of 10 Hz stimulation resulted in a fall in ATP concentration of ~0.4 mM. The [ATP] then recovered towards its baseline level approximately exponentially, with a time constant of ~8.4 min (9.4 min in oligomycin and 7.4 min in 2-deoxyglucose, obtained by fitting the data in fig. 3B of Rangaraju *et al.* 2014), presumably as ATP was resynthesised (if synthesis was incompletely blocked) or ATP diffused into the synaptic terminals from further along the axon. Rangaraju *et al.* (2014) found that ~70% of the initial fall of ATP concentration was dependent on the presence of external calcium, suggesting that ~30% of the ATP used initially may go on pumping out the Na^+ that generates the action potential, whereas the remaining 70% reflects ATP used on calcium pumping or on the vesicle release and recycling that is triggered by Ca^{2+} entry. Knockdown of the SNARE-associated protein Munc13, which controls vesicle release, did not significantly affect presynaptic Ca^{2+} entry or the initial fall of [ATP] evoked by stimulation, consistent with most of the immediate Ca^{2+}-dependent ATP use being on Ca^{2+} extrusion, but greatly speeded the recovery of [ATP] after stimulation, which then recovered with a time constant of ~1.8 min (from fitting the 2-deoxyglucose data in fig. 4C of Rangaraju *et al.* 2014). Thus, after stimulation, there was a prolonged period of ATP consumption that was removed when Munc13 was knocked down, and Munc13 also raised the basal level of [ATP], both of which are consistent with a significant late energy use on vesicle cycling (Rangaraju *et al.* 2014).

With some simple assumptions, we can use the data of Rangaraju *et al.* (2014) to quantify the amount of ATP used on presynaptic Na^+ pumping, Ca^{2+} pumping and vesicle cycling. If we assume that the fast recovery of [ATP] with Munc13 knocked down reflects the time course of resynthesis of ATP by residual unblocked glycolysis and oxidative phosphorylation, or by equilibration of synaptic terminal [ATP] with the [ATP] further away from the terminal (after an initial rapid consumption of ATP on Na^+ and Ca^{2+} pumping), we can estimate the parameters controlling this recovery of [ATP]. Specifically, if the synaptic terminal volume is V, and ATP is resynthesised, or enters the terminal, at a rate $P([ATP]_{axon} - [ATP]_{terminal})$, proportional to its concentration difference from the normal axonal value, $[ATP]_{axon}$, where the ATP production or permeability term P represents synthesis or diffusion into the terminal per concentration difference, then:

$$Vd[ATP]_{terminal}/dt = P([ATP]_{axon} - [ATP]_{terminal})$$

the solution to which is $\Delta[ATP](t) = \Delta[ATP](t = 0)exp\ (-t/\tau)$. where $\Delta[ATP](t)$ is the deviation of [ATP] from its initial value, and $\tau = V/P = 1.8$ min from the data of Rangaraju

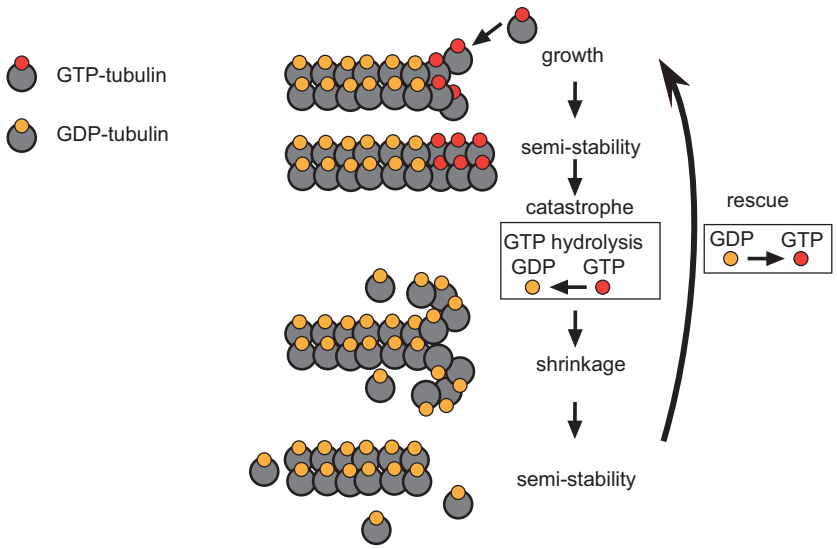

Figure 3. The stages of GTP-dependent dynamic instability in microtubules
Tubulin molecules binding GTP attach to an existing filament and form a semi-stable GTP cap. Subsequently, a 'catastrophe' involving hydrolysis (to GDP) of the bound GTP occurs, which leads to the detachment of individual heterodimers and thus the sudden shrinkage of the microtubule strand. In the 'rescue', GDP is then exchanged for GTP at individual free heterodimers, which are then ready to be re-added to the semi-stable shrunken filament.

et al. (2014) with Munc13 knocked down. When Munc13 is not knocked down, if the prolonged ATP use on vesicle cycling after the stimulation is $U(t)$ mol s^{-1}, then:

$$Vd[\mathrm{ATP}]_{\mathrm{terminal}}/dt = P([\mathrm{ATP}]_{\mathrm{axon}} - [\mathrm{ATP}]_{\mathrm{terminal}}) - U(t)$$

so we can obtain the ATP use on vesicle cycling (in mol min^{-1} m^{-3} or mM min^{-1}) as:

$$U(t)/V = ([\mathrm{ATP}]_{\mathrm{axon}} - [\mathrm{ATP}]_{\mathrm{terminal}})/\tau - d[\mathrm{ATP}]_{\mathrm{terminal}}/dt$$

Because $[\mathrm{ATP}]_{\mathrm{axon}} - [\mathrm{ATP}]_{\mathrm{terminal}} = (0.4\mathrm{mM})\exp(-t/T)$ where $T = 8.4$ min, from Rangaraju *et al.* (2014), it follows that:

$$U(t)/V = (0.175\ \mathrm{mM\ min^{-1}})exp(-t/8.4\ \mathrm{min})$$

so that the total ATP consumed on vesicle cycling is:

$$\int_0^\infty U(t)/Vdt = 1.47\ \mathrm{mM}$$

which is almost 4-fold larger than the initial 0.4 mM fall of [ATP] that we attribute to Na^+ pumping (0.12 mM) and Ca^{2+} pumping (0.28 mM). Thus, actin-related ATP use (nominally 'housekeeping') may be a significant ATP consumer underlying presynaptic signalling.

How many ATP molecules do these values correspond to and how does the presynaptic ATP use on vesicle cycling compare with postsynaptic signalling energy use? Because the stimulation used by Rangaraju *et al.* (2014) employed 600 stimuli, if each stimulus evokes an action potential, then the 0.4 mM initial fall of [ATP] plus the later 1.47 mM used on vesicle cycling implies a total presynaptic ATP use per action potential of (1.87 mM)/600 = 3.12 μM. As the volume of a presynaptic hippocampal bouton is $\sim$0.13 μm^3 (Shepherd & Harris, 1998) or 1.3×10^{-16} l, the use of ATP per bouton per action potential is 4.06×10^{-22} mol, or 244 ATP molecules. Assuming that the same fall of ATP concentration occurs in the short axon segment between two *en passant* boutons in hippocampus *in vivo* (Rangaraju *et al.* (2014) worked on hippocampal area CA3-CA1 cultures), which has a typical length of 5 μm and diameter of 0.2 μm (Li *et al.* 1994; Shepherd & Harris, 1998), and adding the decrease of ATP amount in that volume to the calculation above, gives the result that in total $\sim$540 molecules of ATP are used per bouton and associated axon volume per action potential: 35 on Na^+ pumping, 81 on Ca^{2+} pumping and 424 on vesicle cycling. [A slightly larger, but similar order of magnitude, consumption of ATP is expected for neocortex, if the same fall of [ATP] occurs in *en passant* synaptic terminals (which are more common than terminal boutons: Anderson *et al.* 2002), which have a larger mean volume than in hippocampus (0.35 μm^3: Nava *et al.* 2014) and perhaps a slightly larger inter-bouton distance (4.5 μm, Hellwig *et al.* 1994; 6.4 μm, Stettler *et al.* 2006; 10.5 μm, Anderson *et al.* 2002) and axonal diameter (0.3 μm, Hellwig *et al.* 1994)].

Interestingly, the use of 35 ATP molecules ascribed to Na^+ pumping is 260-fold lower than the ATP that would be needed to extrude the minimal amount of Na^+ needed to polarise the area ($\sim$4.4 μm^2) of the bouton and inter-bouton axon by the 100 mV voltage change of the action potential. This suggests either that the high frequency stimulus train used in these experiments rapidly raises $[Na^+]_i$ sufficiently to saturate the Na^+/K^+ pump, so that the full ATP use on Na^+ pumping occurs over a much longer period than [ATP] was monitored for and is not detected, or that not all of the 600 stimuli evoke action potentials. The use of 81 ATP molecules per action potential to extrude calcium is also much less than the estimate of Attwell & Laughlin (2001) proposing that 3000 ATP molecules are spent on reversing the Ca^{2+} entering per action potential (for a typical release probability of 0.25 and 12,000 ATP used per vesicle released), whereas the use of 424 ATP molecules on vesicle cycling is quite close to the estimate of Attwell & Laughlin (2001) proposing that 821 ATP molecules are expended on vesicle cycling per vesicle released. Interestingly, although Rangaraju *et al.* (2014) report a larger ATP usage on vesicle cycling than on ion pumping presynaptically, this usage constitutes only 1% of the total energy use evoked at synapses per action potential (mainly expended on postsynaptic ion pumping), which Attwell & Laughlin (2001) estimated as being (163,800 ATP molecules per vesicle released) $\times$ (a release probability of 0.25) or 41,000 ATP molecules.

Microtubules use energy by turning over in dynamic instability

Similar to the actin cytoskeleton, microtubules are dynamically unstable (Fig. 3), adding and discarding tubulin as they rearrange their filaments via faster-polymerising plus and slower-polymerising minus ends (Vorobjev *et al.* 1999; Kline-Smith & Walczak, 2004). After the addition of a new α/β-tubulin heterodimer to the microtubule strand, GTP bound to the β component of each heterodimer becomes hydrolysed and the resulting GDP remains bound to the heterodimer (Margolis, 1981; Kline-Smith & Walczak, 2004). However, microtubules do not simply treadmill like actin filaments, which shrink primarily at one end and grow at the other; instead, their ends vacillate between growth and sudden shrinkage events (Mitchison & Kirschner, 1984). GTP-bound heterodimers stabilise the end of a microtubule filament until the GTP is hydrolysed, which

enables depolymerisation. Structural changes such as curving of the subunits after GTP hydrolysis probably also mechanically facilitate depolymerisation (Kueh & Mitchison, 2009).

At present, we lack an accurate quantitative assessment of the amount of ATP used on microtubule turnover. However, tubulin is estimated to be present in brain at ~1.4 g (kg brain)$^{-1}$ (Murphy & Hiebsch, 1979), or 25 μM (using the molecular weight of 55 kDa). Fluorescence recovery after photobleaching experiments suggest that tubulin turns over in microtubules much slower than actin does in the cytoskeleton, on a time scale of the order of 1 h (Edson *et al.* 1993). A calculation similar to that given above for actin turnover implies that the GTP (equivalent to ATP) used on this process will thus be (if essentially all the tubulin is in microtubules) ~25 μM/3600 s = 7 nM s^{-1} (i.e. far less than was estimated for actin cycling above).

Actin and microtubule cycling may be high in microglia

Actin and microtubule cycling as well as the sodium-potassium ATPase are present in all eukaryotic cells. In the brain, however, a distinct class of highly motile cells could place a special strain on the brain's energy budget. Microglia, the macrophages and immune cells of the brain, are far from stationary even in their default 'resting' form (Fig. 4): their processes constantly move through the brain parenchyma to scan for abnormalities and make contact with synapses and neuronal somata (Nimmerjahn *et al.* 2005; Li *et al.* 2012). After tissue damage causes the release of ATP, microglia also extend processes and migrate to the site of injury (Stence *et al.* 2001; Davalos *et al.* 2005). This locomotion is controlled by $P2Y_{12}$ receptors (Haynes *et al.* 2012). They also change their shape and retract their processes to phagocytose cells and other debris, which is an actin-based process, and travel in response to UDP signals released by cells ready for phagocytosis (Koizumi *et al.* 2007). It is not known whether microglial motility and phagocytosis are powered by glycolytic pathways or via oxidative phosphorylation. However, these tasks are probable contenders for significant energy use by the brain.

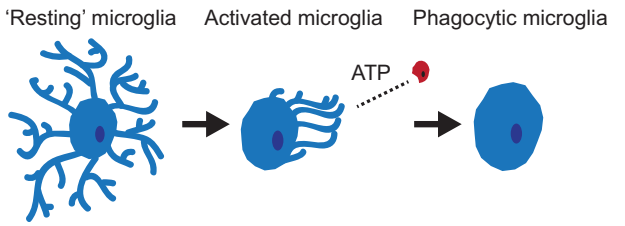

Figure 4. Different stages of microglial morphology depending on their task
All microglial stages, as well as the transitions between them, are highly dependent on actin turnover. In the misleadingly-named 'resting' form, their processes continually move to scan the brain parenchyma, requiring constant restructuring of the actin cytoskeleton. In response to various signals, such as ATP released from damaged cells, microglia become activated. They extend processes towards the site of injury (schematised as a dying cell in red) and retract those that were facing away from the damaged area (Davalos *et al*. 2005). Prior to travelling to a site of cell or tissue damage and performing phagocytosis, microglia withdraw their processes entirely and translocate, after the formation of new highly motile protrusions (Stence *et al*. 2001).

Proton leak across the mitochondrial membrane implies a loss of ATP production

Mitochondria use more oxygen than is accounted for by oxidative phosphorylation, and even consume it in the absence of ATP synthesis (Nicholls, 1974). This is the result of a continuous proton leak across the mitochondrial membrane, which has been demonstrated in cells of various tissue types, including brain (Rolfe *et al.* 1994; Rolfe & Brown, 1997). From experiments inhibiting cellular respiration and measuring the resulting changes in mitochondrial oxygen consumption, Rolfe & Brown (1997) estimated the overall contribution of mitochondrial proton leak to the resting metabolic rate to be ~20% across a range of organs and tissues.

Proteins and phospholipids synthesis and turnover consume ATP

Dunlop *et al.* (1994) measured protein turnover in the young adult rat brain to be 0.65% h^{-1}. The brain protein content for adult rats is ~100 mg g^{-1} (Pitts & Quick, 1967) and the formation of a peptide bond requires four molecules of ATP. Because the amino acid associated with each peptide bond has an average molecular weight of 110 (Rolfe & Brown, 1997), the number of moles of amino acid turned over per unit time can be calculated to be 9.84 × 10^{-8} mol g^{-1} min^{-1}. Multiplication by four molecules of ATP gives the turnover of ATP as 0.39 μmol g^{-1} min^{-1}, which can then be compared to the whole-brain usage of 31 μM ATP g min^{-1} (Sokoloff *et al.* 1997). By this estimate, protein synthesis accounts for no more than ~1.3% of total brain ATP consumption (Rolfe & Brown, 1997; Attwell & Laughlin, 2001). In the rabbit retina, Ames (2000) also estimated a low (1.3%) contribution of protein synthesis to the global energy budget of the retina, and even less for nucleic acid (0.7%) and phospholipid (0.6%) synthesis.

However, phospholipid turnover has been a long-underestimated component of the brain's energy consumption: along with Ames's calculation, early

estimates allocated ∼2% of the brain's net ATP use to this process (McKenna *et al.* 2012). Contradicting this, Purdon & Rapoport (1998) showed that, because the half-lives of fatty acids used to build up phospholipids are much shorter than had previously been accounted for, their recycling and re-incorporation into phospholipids may be responsible for 5% of ATP consumed in the brain. Furthermore, cellular lipid bilayers require continuous maintenance of the asymmetric distribution of aminophospholipids. The transport of phospholipids through the bilayer is carried out by the aminophospholipid translocase, consuming 1 ATP molecule per phospholipid transferred (Beleznay *et al.* 1993; Diaz & Schroit, 1996). Purdon and Rapoport (1998) calculated that 8% of net ATP consumption is spent on this maintenance of asymmetry. Thus, excluding *de novo* lipid synthesis, ∼13% of the brain's ATP reserves might be spent on phospholipid-related reactions. Taking *de novo* synthesis into account, Purdon & Rapoport (2007) subsequently estimated an even higher fraction of brain ATP usage, namely 25%, to be spent on phospholipid metabolism, with maintenance of the phospholipids' phosphorylation state (12%), the upkeep of aminophospholipid asymmetries (7.7%) and fatty acid turnover inside phospholipids (5%) being the most energy-expensive components.

The energy budget is altered in pathology

Cerebral ischaemia, or restricted blood supply to the brain, leads to glucose and oxygen depletion, preventing energy use in the core of the lesion and causing stroke. Reduced availability of ATP, accumulation of fatty acid and divalent ions inside cells, and degradation of the sodium-potassium pump's phospholipid components during and directly after ischaemia all lead to inhibition of the sodium-potassium pump (Lees, 1991) and a run-down of transmembrane ion gradients. This not only results in a greater need for ATP to re-establish the ionic distributions across the lipid bilayer when blood flow is restored after ischaemia, but also evokes a reversal of glutamate transporters (Rossi *et al.* 2000). The glutamate released will evoke a Na^+ influx into neurons and so exacerbate energy depletion caused by ion pumping (Ye *et al.* 2010),

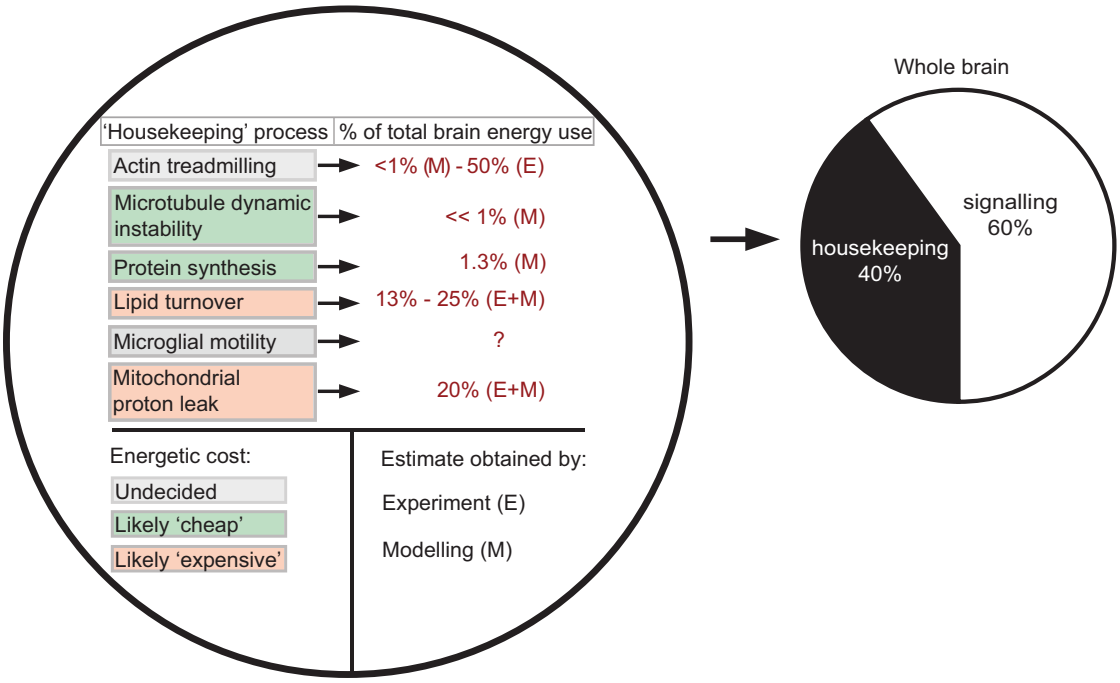

Figure 5. An updated tentative summary of the brain's non-signalling energy expenditure
Current theoretical estimates and experimental data assessing the contribution of each 'housekeeping' process to the brain's total energy budget are inconclusive for many processes, varying widely in some cases. Further research is needed to fill these gaps, and the 40% value shown (right), for the whole brain according to Astrup *et al*. (1981*a*), as opposed to the 25% assumed for grey matter in Fig. 1, is quite uncertain. Left: estimates for each 'housekeeping' process' percentage share of total brain energy expenditure are given as a summary of this review. E, data for the estimate were obtained experimentally; M, an estimate was calculated from models based on experimental data (often from several animal models, ages, etc.); E + M a combination, where a relatively small leap from experimental data to the final estimate was required. For quick reference, processes are labelled as energetically inexpensive (green), expensive (orange) or of as yet uncertain energy consumption because of contradictory evidence or a lack of data (grey).

and also activates a large neurotoxic influx of calcium into cells, mainly through NMDA receptors. A similar but smaller inhibition of the sodium-potassium pump is present in hypoglycaemia and during seizures (Lees, 1991).

Ischaemia, and other events where DNA strand breaks are common, lead to an activation of PARP to repair damaged DNA. This results in an intracellular depletion of the PARP substrate NAD^+ and in turn of ATP, which is consumed in an attempt to maintain NAD^+ levels. Ultimately, this may lead to cell death by necrosis. At the same time, activation of PARP prevents energy-intensive apoptosis (Ha & Snyder, 2000; Pacher & Szabo, 2008). The depletion of energy therefore has profound consequences for degeneration after ischaemic events: ATP depletion can cause ongoing apoptosis to transform into necrosis, although neuronal death after stroke may be reduced by inhibiting the PARP pathway. On the other hand, Ha & Snyder (2000) speculated that ATP depletion caused by PARP activation could be beneficial during physiological (non-excessive) DNA repair because cells could be forced to remain in a low-activity mode when repairs are in progress. To answer the question of how such an energy-depleted state affects cells' information processing capabilities, further research is needed.

Microglial activity is also highly upregulated in ischaemia. After a transient restriction of blood supply, a large number of activated microglia travel to the site of injury. They can not only exert a neuroprotective function (Lalancette-Hébert *et al.* 2007), but also are involved in restructuring neuronal circuits by eliminating synapses in the ischaemic area, prolonging their contact with these synapses from a few minutes to up to 1 h (Wake *et al.* 2009). All of these processes are probably energy-intensive.

Cortical spreading depression (CSD), a feature of migraine, traumatic brain injury and stroke, is another pathology that alters energy supply and usage in the brain (Piilgaard & Lauritzen, 2009). After inducing CSD in the cortex of anaesthetised rats, Piilgaard & Lauritzen (2009) found a dramatic increase in the rate of cerebral blood flow (CBF) and the cerebral metabolic rate of oxygen ($CMRO_2$) lasting a few minutes after induction. This was followed by a smaller but prolonged (>1 h) increase of oxygen consumption and decrease of blood flow, the combination of which resulted in tissue hypoxia. The elevated energy consumption can be explained by the need to restore ion gradients that had run down during CSD. In the first minutes after CSD, additional oxygen is also required for the oxidation of accumulated lactate and for re-synthesis of glycogen from glucose residues. After their levels have returned to normal, continuing high oxygen consumption may be linked to the use of oxygen in decreasing intermediate metabolic pools resulting from glucose metabolism (Madsen *et al.* 1999; Piilgaard & Lauritzen, 2009).

Ageing has also been shown to fundamentally change the interplay of CBF and $CMRO_2$. The signalling systems controlling CBF change with age (Harris *et al.* 2011). In a re-analysis of a previous positron emission tomography study in humans, Aanerud *et al.* (2012) found a decline of CBF with age in much of the cortex (but not in primary sensory-motor and occipital cortices or subcortical structures), possibly because the capillary density declines with age (Brown & Thore, 2011). Although the oxygen extraction fraction increased with age, this was not sufficient to prevent a decrease in $CMRO_2$ (Aanerud *et al.* 2012). These changes were already apparent when middle-aged and young brains were compared, and increased further between middle and old age. Contradicting this, however, Peng *et al.* (2014) measured an increase of oxygen consumption with age using magnetic resonance imaging. They attributed this effect to a loss of neurons with age, so that the remaining neurons have to expend more energy to compensate for this loss and remain equally functional. Neuronal efficiency could also be reduced, and mitochondrial proton leak might be increased as mitochondrial functionality declines with age. These conflicting results might perhaps be reconciled because Aanerud *et al.* (2012) primarily measured regional changes in the metabolic rate of oxygen, whereas Peng *et al.* (2014) took a global measure of oxygen use that did not distinguish between grey and white matter, where different changes may occur. In summary, what happens to the brain's energy supply during ageing is still controversial, and it is still largely undetermined whether these changes differentially affect particular components of the brain's energy budget.

Finally, Alzheimer's disease profoundly alters energy provision and consumption in the brain. De la Torre (1993) hypothesised that Alzheimer's disease might be the result of a slight long-term mismatch between cerebral energy supply and demand, which leads to energy deprivation. Indeed, patients with Alzheimer's disease exhibit decreased CBF in brain areas affected by Alzheimer's pathology (Asllani *et al.* 2008). However, other studies on dementia patients found a CBF increase in some brain areas and a decrease in others (Dai *et al.* 2009). Neuronal energy production is also affected in Alzheimer's disease because mitochondrial dysfunction is an early feature of the pathology (McInnes, 2013). Furthermore, signalling from neurons to the vasculature can be impaired (Rancillac *et al.* 2012). However, because plaques can form around blood vessels, decreased vascular reactivity and mismatched blood flow could be a consequence rather than a cause of Alzheimer's disease (Weller *et al.* 2008; Niwa *et al.* 2001). Non-signalling processes are also affected by Alzheimer's disease because the creation of tau tangles could destabilise microtubules, with which tau is associated (Lee & Trojanowski, 1992). Microglia can be

activated by β-amyloid and its precursor protein (Meda *et al.* 1995; Barger & Harmon, 1997), which will alter their motility and energy demands. Turnover of the actin cytoskeleton is also changed by β-amyloid. For example, the protein cofilin which is involved in the disassembly of actin is upregulated, whereas stabilising proteins are downregulated, resulting in a disruption of the actin cytoskeleton, which may facilitate the loss of dendritic spines and ultimately synapses (Penzes & VanLeeuwen, 2011).

Discussion

From the many experiments using the sodium pump blocker ouabain in brain slices or *in vivo*, it has become clear that, although electrical signalling associated with a Na^+ influx consumes a significant part of the brain's energy expenditure, a large share of brain energy use remains unaccounted for and is not directly related to signalling. There are several mechanisms that probably contribute to the unexplained energy use. The actin and microtubule cytoskeletons are highly dynamic, even in cells at rest, and their turnover is ATP- and GTP-dependent. Proteins and phospholipids are synthesised and an asymmetrical distribution of phospholipids across the lipid bilayer is maintained. Proton leak occurs across mitochondrial membranes, and highly motile microglia surveying the brain and responding to injury require energy resources to do so. Data have been gathered or models have been made for some of these processes (e.g. estimates of the energy spent on 'housekeeping' processes are related to whole-brain energy use in Fig. 5); however, defining the absolute share of each 'housekeeping' process in the brain's energy budget requires further research. The experiments surveyed in this review use different animal models or experimental protocols, and have been carried out at various ages, leading to divergent results. This increases uncertainty when building an energy budget based on experimental data or by modelling energy-consuming processes. Therefore, it is crucial that gaps in our knowledge of different parameters (e.g. the speed of actin treadmilling) are filled by future research.

From experiments blocking the sodium-potassium pump (Astrup *et al.* 1981*a*), signalling-related events (powered by Na^+ pumping) can be estimated to be responsible for at least 55% of the total brain energy consumption (averaged across grey and white matter). Although it has been suggested that the actin cytoskeleton accounts for the majority of the unexplained energy expenditure (50% of neuronal energy use; Bernstein & Bamburg, 2003), flaws in the experimental procedure used (see above), and our modelling of the ATP usage during actin cycling, undermine this finding, and further experiments will probably lower this value. In the brain, highly motile microglia might account for a disproportionate share of actin cycling, although, as noted above, we have used the data of Rangaraju *et al.* (2014) to show that presynaptic ATP-consuming cytoskeletal events mediating vesicle recycling use less than 1% of the ATP calculated to be consumed postsynaptically at synapses. No research has yet investigated the energy used by the dynamic instability of microtubules, which in principle could be of a similar order of magnitude to that used on actin turnover, although our approximate estimate (see above) suggests that much less ATP is used on microtubule restructuring than on actin cycling. Proton leak across the mitochondrial membrane has been estimated in isolated mitochondria to consume up to one-fifth of the resting O_2 use, although it is unclear how well this represents the protein leak in intact tissues. Similarly, accurate data are lacking on the energy needed for protein synthesis, which has been estimated theoretically to account for only $\sim$1.3% of the brain's energy use. However, experimental data exist for phospholipid turnover in the brain and for the maintenance of phospholipid asymmetry across the lipid bilayer, and suggest that a relatively high (13–25%) share of the energy budget is used on these processes.

In highly prevalent pathologies such as ischaemia, an upregulation of neuronal and microglial activity occurs in conjunction with a decrease of energy use in the ischaemic core, which probably alters the allocation of the brain's energy budget profoundly. This balance might also be upset in other pathologies, such as CSD, as well as in healthy and pathological ageing and Alzheimer's disease.

Too little is known about how the energy-related consequences of pathologies and ageing affect non-signalling brain functions that depend on a supply of ATP. Although it can be concluded that signalling is not the only task of the brain requiring a large portion of its energy budget, further experiments are required to shed more light on the exact energy usage of the many 'housekeeping' tasks that are just as vital to the brain's functioning, and how they are affected by pathology.

References

Aanerud J, Borghammer P, Chakravarty MM, Vang K, Rodell AB, Jónsdottir KY, Møller A, Ashkanian M, Vafaee MS, Iversen P, Johannsen P & Gjedde A (2012). Brain energy metabolism and blood flow differences in healthy aging. *J Cereb Blood Flow Metab* **32**, 1177–1187.

Alle H, Roth A, Geiger JR (2009). Energy-efficient action potentials in hippocampal mossy fibers. *Science* **325**, 1405–1408.

Ames A (2000). CNS energy metabolism as related to function. *Brain Res Rev* **34**, 42–68.

Anderson JC, Binzegger T, Douglas RJ & Martin KAC (2002). Chance or design? Some specific considerations concerning symaptic boutons in cat visual cortex. *J. Neurocytol.* **31**, 211–229.

Asllani I, Habeck C, Scarmeas N, Borogovac A, Brown TR & Stern Y (2008). Multivariate and univariate analysis of continuous arterial spin labeling perfusion MRI in Alzheimer's disease. *J Cereb Blood Flow Metab* **28**, 725–736.

Astrup J, Siesjo BK & Symon L (1981). Thresholds in cerebral ischemia - the ischemic penumbra. *Stroke* **12**, 723–725.

Astrup J, Sorensen PM & Sorensen HR (1981a). Oxygen and glucose consumption related to Na^+-K^+ transport in canine brain. *Stroke* **12**, 726–730.

Attwell D & Gibb A (2005). Neuroenergetics and the kinetic design of excitatory synapses. *Nat Rev Neurosci* **6**, 841–849.

Attwell D & Laughlin SB (2001). An energy budget for signaling in the grey matter of the brain. *J Cereb Blood Flow Metab* **21**, 1133–1145.

Barger, SW & Harmon, AD (1997). Microglial activation by Alzheimer amyloid precursor protein and modulation by apolipoprotein E. *Nature*, **388**, 878–881.

Beleznay Z, Zachowski A, Devaux PF, Navazo MP & Ott P (1993). ATP-dependent aminophospholipid translocation in erythrocyte vesicles: stoichiometry of transport. *Biochemistry* **32**, 3146–3152.

Belmont LD & Drubin, DG (1998). The yeast V159N actin mutant reveals roles for actin dynamics in vivo. *J Cell Biol* **142**, 1289–1299.

Bernstein BW & Bamburg JR (2003). Actin-ATP hydrolysis is a major energy drain for neurons. *J Neurosci* **23**, 1–6.

Brown WR & Thore CR (2011). Review: cerebral microvascular pathology in ageing and neurodegeneration: cerebral microvascular pathology. *Neuropathol Appl Neurobiol* **37**, 56–74.

Carlier M-F & Pantaloni D (1997). Control of actin dynamics in cell motility. *J Mol Biol* **269**, 459–467.

Carlier M-F, Pantaloni D, Evans JA, Lambooy PK, Korn ED & Webb MR (1988). The hydrolysis of ATP that accompanies actin polymerization is essentially irreversible. *FEBS Letters* **235**, 211–214.

Condeelis J (1993). Life at the leading edge: the formation of cell protrusions. *Annu Rev Cell Biol* **9**, 411–444.

Dai W, Lopez OL, Carmichael OT, Becker JT, Kuller LH & Gach HM (2009). Mild cognitive impairment and Alzheimer disease: patterns of altered cerebral blood flow at MR imaging. *Radiology* **250**, 856–866.

Davalos D, Grutzendler J, Yang G, Kim JV, Zuo Y, Jung S, Littman DR, Dustin ML & Gan W-B (2005). ATP mediates rapid microglial response to local brain injury in vivo. *Nat Neurosci* **8**, 752–758.

Dela Torre JC & Mussivand T (1993). Can disturbed brain microcirculation cause Alzheimer's disease? *Neurol Res* **15**, 146–153.

Devineni N, Minamide LS, Niu M, Safer D, Verma R, Bamburg JR & Nachmias VT (1999). A quantitative analysis of G-actin binding proteins and the G-actin pool in developing chick brain. *Brain Res* **823**, 129–140.

Diaz C & Schroit AJ (1996). Role of translocases in the generation of phosphatidylserine asymmetry. *J Membr Biol* **151**, 1–9.

Dunlop DS, Yang X-R & Lajtha A (1994). The effect of elevated plasma phenylalanine levels on protein synthesis rates in adult rat brain. *Biochem J* **302**, 601–610.

Edson KJ, Lim S-S, Borisy GG & Letourneau PC (1993). FRAP analysis of the stability of the microtubule population along the neurites of chick sensory neurons. *Cell Motil Cytoskeleton* **25**, 59–72.

Fowler JC (1990). Adenosine antagonists alter the synaptic response to in vitro ischemia in the rat hippocampus. *Brain Res* **509**, 331–334.

Fowler JC (1993*a*). Changes in extracellular adenosine levels and population spike amplitude during graded hypoxia in the rat hippocampal slice. *Naunyn Schmiedebergs Arch Pharmacol* **347**, 73–78.

Fowler JC (1993*b*). Purine release and inhibition of synaptic transmission during hypoxia and hypoglycemia in rat hippocampal slices. *Neurosci Lett* **157**, 83–86.

Fünfschilling U, Supplie LM, Mahad D, Boretius S, Saab AS, Edgar J, Brinkmann BG, Kassmann CM, Tzvetanova ID, Möbius W, Diaz F, Meijer D, Suter U, Hamprecht B, Sereda MW, Moraes CT, Frahm J, Goebbels S & Nave K-A (2012). Glycolytic oligodendrocytes maintain myelin and long-term axonal integrity. *Nature* **485**, 517–521.

Graham B & Redman S (1994). A simulation of action potentials in synaptic boutons during presynaptic inhibition. *J Neurophysiol* **71**, 538–538.

Ha H & Snyder S (2000). Poly(ADP-ribose) Polymerase-1 in the nervous system. *Neurobiol Dis* **7**, 225–239.

Hall A (1998). Rho GTPases and the actin cytoskeleton. *Science* **279**, 509–514.

Hallermann S, deKock CPJ, Stuart GJ & Kole MHP (2012). State and location dependence of action potential metabolic cost in cortical pyramidal neurons. *Nat Neurosci* **15**, 1007–1014.

Harris JJ & Attwell D (2012). The energetics of CNS white matter. *J Neurosci* **32**, 356–371.

Harris JJ, Reynell C & Attwell D (2011). The physiology of developmental changes in BOLD functional imaging signals. *Dev Cogn Neurosci* **1**, 199–216.

Haynes SE, Hollopeter G, Yang G, Kurpius D, Dailey ME, Gan W-B & Julius D (2006). The P2Y12 receptor regulates microglial activation by extracellular nucleotides. *Nat Neurosci* **9**, 1512–1519.

Hellwig B, Schüz A & Aertsen A (1994). Synapses on axon collaterals of pyramidal cells are spaced at random intervals: a Golgi study in the mouse cerebral cortex. *Biol Cybern* **71**, 1–12.

Kety SS (1957). The general metabolism of the brain in vivo. In *Metabolism of the nervous system*, ed. Richter D, pp. 221–237. Pergamon, London.

Kline-Smith SL & Walczak CE (2004). Mitotic spindle assembly and chromosome segregation. *Mol Cell* **15**, 317–327.

Koizumi S, Shigemoto-Mogami Y, Nasu-Tada K, Shinozaki Y, Ohsawa K, Tsuda M, Joshi BV, Jacobson KA, Kohsaka S & Inoue K (2007). UDP acting at P2Y6 receptors is a mediator of microglial phagocytosis. *Nature* **446**, 1091–1095.

Kueh HY & Mitchison TJ (2009). Structural plasticity in actin and tubulin polymer dynamics. *Science* **325**, 960–963.

Lalancette-Hebert M, Gowing G, Simard A, Weng YC & Kriz J (2007). Selective ablation of proliferating microglial cells exacerbates ischemic injury in the brain. *J Neurosci* **27**, 2596–2605.

Latini S, Bordoni F, Corradetti R, Pepeu G & Pedata F (1998). Temporal correlation between adenosine outflow and synaptic potential inhibition in rat hippocampal slices during ischemia-like conditions. *Brain Res.* **794**, 325–328.

Laughlin SB & Sejnowski, TJ (2003). Communication in neuronal networks. *Science* **301**, 1870–1874.

Lee VM-Y & Trojanowski JQ (1992). The disordered neuronal cytoskeleton in Alzheimer's disease. *Curr Opin Neurobiol* **2**, 653–656.

Lees GJ (1991). Inhibition of sodium-potassium-ATPase: a potentially ubiquitous mechanism contributing to central nervous system neuropathology. *Brain Res Rev* **16**, 283–300.

Lennie P (2003). The cost of cortical computation. *Curr Biol* **13**, 493–497.

Li X-G, Somogyi P, Ylinen A & Buzsáki G (1994). The hippocampal CA3 network: an in vivo intracellular labeling study. *J Comp Neurol* **339**, 181–208.

Li Y, Du X, Liu C, Wen Z & Du J (2012). Reciprocal regulation between resting microglial dynamics and neuronal activity in vivo. *Dev Cell* **23**, 1189–1202.

Madsen PL, Cruz NF, Sokoloff L & Dienel GA (1999). Cerebral oxygen/glucose ratio is low during sensory stimulation and rises above normal during recovery: excess glucose consumption during stimulation is not accounted for by lactate efflux from or accumulation in brain tissue. *J Cereb Blood Flow Metab* **19**, 393–400.

Margolis RL (1981). Role of GTP hydrolysis in microtubule treadmilling and assembly. *Proc Natl Acad Sci U S A* **78**, 1586–1590.

McInnes J (2013). Insights on altered mitochondrial function and dynamics in the pathogenesis of neurodegeneration. *Transl Neurodegener* **2**, 12.

McKenna MC, Dienel GA, Sonnewald U, Waagepetersen H & Schousboe A (2012). Energy metabolism of the brain. In *Basic neurochemistry: molecular, cellular and medical aspects*, 8th edn, ed. Siegel GJ, Agranoff BW, Albers RW & Molinoff MD, p 202. Raven Press, New York , NY.

Meda L, Cassatella MA, Szendrei GI, Otvos L Jr, Baron P, Villalba M, Ferrari D & Rossi F (1995). Activation of microglial cells by beta-amyloid protein and interferon gamma. *Nature* **374**, 647–650.

Mitchison T & Kirschner M (1984). Dynamic instability of microtubule growth. *Nature* **312**, 237–242.

Murphy DB & Hiebsch RR (1979). Purification of microtubule protein from beef brain and comparison of the assembly requirements for neuronal microtubules isolated from beef and hog. *Anal Biochem* **96**, 225–235.

Nava N, Chen F, Wegener G, Popoli M & Nyengaard JR (2014). A new efficient method for synaptic vesicle quantification reveals differences between medial prefrontal cortex perforated and nonperforated synapses. *J Comp Neurol* **522**, 284–297.

Nave K-A (2010). Myelination and support of axonal integrity by glia. *Nature* **468**, 244–252.

Nicholls DG (1974). The influence of respiration and ATP hydrolysis on the proton-electrochemical gradient across the inner membrane of rat-liver mitochondria as determined by ion distribution. *Eur J Biochem* **50**, 305–315.

Nimmerjahn A, Kirchhoff F & Helmchen, F (2005). Resting microglial cells are highly dynamic surveillants of brain parenchyma in vivo. *Science* **308**, 1314–1318.

Niven JE & Laughlin SB (2008). Energy limitation as a selective pressure on the evolution of sensory systems. *J Exp Biol* **211**, 1792–1804.

Niwa K, Porter VA, Kazama K, Cornfield D, Carlson GA & Iadecola C (2001). Aß-peptides enhance vasoconstriction in cerebral circulation. *Am J Physiol Heart Circ Physiol* **281**, H2417–H2424.

Pacher P & Szabo C (2008). Role of the peroxynitrite-poly(ADP-ribose) polymerase pathway in human disease. *Am J Pathol* **173**, 2–13.

Pantaloni D, LeClainche C & Carlier, M-F (2001). Mechanism of actin-based motility. *Science* **292**, 1502–1506.

Pathania M, Davenport EC, Muir J, Sheehan DF, López-Doménech G & Kittler JT (2014). The autism and schizophrenia associated gene CYFIP1 is critical for the maintenance of dendritic complexity and the stabilization of mature spines. *Transl Psychiatry* **4**, 1–11.

Pellerin L & Magistretti PJ (1994). Glutamate uptake into astrocytes stimulates aerobic glycolysis: a mechanism coupling neuronal activity to glucose utilization. *Proc Natl Acad Sci U S A* **91**, 10625–10629.

Peng S-L, Dumas JA, Park DC, Liu P, Filbey FM, McAdams CJ, Pinkham AE, Adinoff B, Zhang R & Lu H (2014). Age-related increase of resting metabolic rate in the human brain. *NeuroImage* **98**, 176–183.

Penzes P & VanLeeuwen J-E (2011). Impaired regulation of synaptic actin cytoskeleton in Alzheimer's disease. *Brain Res Rev* **67**, 184–192.

Piilgaard H & Lauritzen M (2009). Persistent increase in oxygen consumption and impaired neurovascular coupling after spreading depression in rat neocortex. *J Cereb Blood Flow Metab* **29**, 1517–1527.

Pitts FN & Quick C (1967). Brain succinate semialdehyde dehydrogenase-II. Changes in the developing rat brain. *J Neurochem* **14**, 561–570.

Pollard TD, Blanchoin L & Mullins RD (2000). Molecular mechanisms controlling actin filament dynamics in nonmuscle cells. *Annu Rev Biophys Biomol Struct* **29**, 545–576.

Pollard TD & Borisy GG (2003). Cellular motility driven by assembly and disassembly of actin filaments. *Cell* **112**, 453–465.

Purdon A & Rapoport S (1998). Energy requirements for two aspects of phospholipid metabolism in mammalian brain. *Biochem J* **335**, 313–318.

Purdon A & Rapoport S (2007). Energy consumption by phospholipid metabolism in mammalian brain. In *Handbook of neurochemistry and molecular neurobiology: brain energetics. Integration of molecular and cellular processes*, ed. Lajtha A, Gibson GE & Dienel GA, pp. 402–427. Springer, New York , NY.

Rancillac A, Geoffroy H & Rossier J (2012). Impaired neurovascular coupling in the APPxPS1 mouse model of Alzheimer's disease. *Curr Alzheimer Res* **9**, 1221–1230.

Rangaraju V, Calloway N & Ryan TA (2014). Activity-driven local ATP synthesis is required for synaptic function. *Cell* **156**, 825–835.

Rolfe DF & Brown GC (1997). Cellular energy utilization and molecular origin of standard metabolic rate in mammals. *Physiol Rev* **77**, 731–758.

Rolfe DF, Hulbert AJ & Brand MD (1994). Characteristics of mitochondrial proton leak and control of oxidative phosphorylation in the major oxygen-consuming tissues of the rat. *Biochim Biophys Acta* **1118**, 405–416.

Rossi DJ, Oshima T & Attwell D (2000). Glutamate release in severe brain ischaemia is mainly by reversed uptake. *Nature* **403**, 316–321.

Sankaranarayanan S, Atluri PP & Ryan TA (2003). Actin has a molecular scaffolding, not propulsive, role in presynaptic function. *Nat Neurosci* **6**, 127–135.

Shepherd GM & Harris KM (1998). Three-dimensional structure and composition of CA3→CA1 axons in rat hippocampal slices: implications for presynaptic connectivity and compartmentalization. *J Neurosci* **18**, 8300–8310.

Shibuki K (1989). Calcium-dependent and ouabain-resistant oxygen consumption in the rat neurohypophysis. *Brain Res* **487**, 96–104.

Shupliakov O, Bloom O, Gustafsson JS, Kjaerulff O, Low P, Tomilin N, Pieribone VA, Greengard P & Brodin L (2002). Impaired recycling of synaptic vesicles after acute perturbation of the presynaptic actin cytoskeleton. *Proc Natl Acad Sci U S A* **99**, 14476–14481.

Sibson NR, Dhankhar A, Mason GF, Rothman DL, Behar KL & Shulman RG (1998). Stoichiometric coupling of brain glucose metabolism and glutamatergic neuronal activity. *Proc Natl Acad Sci* **95**, 316–321.

Star EN, Kwiatkowski DJ & Murthy VN (2002). Rapid turnover of actin in dendritic spines and its regulation by activity. *Nat Neurosci* **5**, 239–246.

Stence N, Waite M & Dailey ME (2001). Dynamics of microglial activation: a confocal time-lapse analysis in hippocampal slices. *Glia* **33**, 256–266.

Sokoloff L (1960). The metabolism of the central nervous system in vivo. In *Handbook of physiology-neurophysiology*, 3rd edn, ed. Field J, Magoun HW & Hall VE, pp. 1843–1864. American Physiological Society, Washington , DC.

Sokoloff L, Reivich M, Kennedy C, Rosiers MHD, Patlak CS, Pettigrew KD, Sakurada O & Shinohara M (1977). The [^{14}C]deoxyglucose method for the measurement of local cerebral glucose utilization: theory, procedure, and normal values in the conscious and anesthetized albino rat. *J Neurochem* **28**, 897–916.

Stettler DD, Yamahachi H, Li W, Denk W & Gilbert CD (2006). Axons and synaptic boutons are highly dynamic in adult visual cortex. *Neuron* **49**, 877–887.

Urban NT, Willig KI, Hell SW & Nägerl UV (2011). STED nanoscopy of actin dynamics in synapses deep inside living brain slices. *Biophys J* **101**, 1277–1284.

Vorobjev IA, Rodionov VI, Maly IV & Borisy GG (1999). Contribution of plus and minus end pathways to microtubule turnover. *J Cell Sci* **112**, 2277–2289.

Wake H, Moorhouse AJ, Jinno S, Kohsaka S & Nabekura J (2009). Resting microglia directly monitor the functional state of synapses in vivo and determine the fate of ischemic terminals. *J Neurosci* **29**, 3974–3980.

Wegner, A (1976). Head to tail polymerization of actin. *J Mol Biol* **108**, 139–150.

Weller RO, Subash M, Preston SD, Mazanti I & Carare RO (2007). Symposium: clearance of Aβ from the brain in Alzheimer's disease: perivascular drainage of amyloid-β peptides from the brain and its failure in cerebral amyloid angiopathy and Alzheimer's disease. *Brain Pathol* **18**, 253–266.

Whittam, R (1961). The dependence of the respiration of brain cortex on active cation transport. *Biochem J* **82**, 205–212.

Ye H, Jalini S, Zhang L, Charlton M & Carlen PL (2010). Early ischemia enhances action potential-dependent, spontaneous glutamatergic responses in CA1 neurons. *J Cereb Blood Flow Metab* **30**, 555–565.

Additional information

Competing interests

The authors declare that they have no competing interests.

Funding

Supported by the European Research Council, Fondation Leducq and Wellcome Trust. Elisabeth Engl is in the 4th year of her PhD in Neuroscience at University College London.

Acknowledgements

We thank Julia Harris for comments on the paper.